Composites Part A 125 (2019) 105560

Contents lists available at ScienceDirect

Composites Part A

journal homepage: www.elsevier.com/locate/compositesa

Biofabrication of a novel bacteria/bacterial cellulose composite for improved adsorption capacity

Yizao Wan[a,b], Jie Wang[a], Miguel Gama[c], Ruisong Guo[b], Quanchao Zhang[a], Peibiao Zhang[d], Fanglian Yao[e], Honglin Luo[a,b,*]

[a] Institute of Advanced Materials, East China Jiaotong University, Nanchang 330013, China
[b] School of Materials Science and Engineering, Tianjin University, Tianjin 300072, China
[c] Centro de Engenharia Biológica, Universidade do Minho, Campus de Gualtar, P 4715-057 Braga, Portugal
[d] Changchun Institute of Applied Chemistry, Chinese Academy of Sciences, Changchun 130022, China
[e] Key Laboratory of Systems Bioengineering of Ministry of Education, School of Chemical Engineering and Technology, Tianjin University, Tianjin 300072, China

ARTICLE INFO

Keywords:
Bacterial cellulose
Bacteria
Composite
Adsorption
Metal ions

ABSTRACT

Conventional fabrication of bacterial cellulose (BC) involves treatment with hot NaOH aqueous solutions to remove bacteria (BA). Herein, we report a simpler and cheaper method for the preparation of BA/BC composite without alkalization, which keeps the BA in the nanofibrous BC network. Scanning electron microscopy (SEM) observation showed naturally distributed BA in BC matrix with a tightly entangled structure. Such BA-embedded BA/BC composite exhibited improved mechanical strength and modulus over BC. When used as adsorbent, the BA/BC composite exhibited significantly higher adsorption capacities to Pb(II), Cu(II), Ni(II), and Cr(VI) compared to bare BC. The much higher adsorption capacities of BA/BC are due to the presence of functional groups in the BA, such as amide, which are known to be involved in coordination interaction. This breakthrough strategy not only made the fabrication process simpler and more cost-effective, but also produced a new BC-based adsorbent with improved adsorption capacity to heavy metals.

1. Introduction

Cellulose, the most abundant natural polymer on earth, is a low cost, nontoxic, biocompatible, and biodegradable polymer, and has been widely used in various composites [1–3]. Besides cellulose derived from trees, cotton, straw and other plant sources, some Gram-negative species of bacteria (BA) such as *Gluconacetobacter, Acetobacter, Salmonella, Achromobacter, Pseudomonas, Sarcina, Azobacter, Rhizobium, Agrobacterium,* and *Alcaligenes* [4], also produce cellulose, which is named Bacterial Cellulose (BC). When produced in static culture, BC is obtained as a film which may be a few centimeters thick; structurally, it consists of nanofibers ranging from 20 to 100 nm in diameter.

Indeed, unlike plant derived cellulose, employing different chemical treatments is unnecessary to obtain pure cellulose since BC does not contain any other compound present in the plant pulp or from animal origin [5]. However, the untreated BC membrane contains BA. These cell residues as well as other impurities such as organic acids, salts as well as residual sugars and other components in the culture medium should be removed. Although many methods are employed such as washing, centrifugation, filtration, and chemical extraction [4], washing BC with hot NaOH solution is the most commonly used [4–11]. The effect of NaOH treatment on structure and mechanical properties of BC has been reported [8,12]. Obviously, regardless of its effect on BC, employment of NaOH results in potential pollution to the environment and thus the production process is not environmentally friendly.

Based on this consideration, we came up with a new strategy: instead of removing BA using alkaline treatment, we preserve them while removing other fermentation residues through thorough purification. We hypothesize that purifying BC without NaOH may not only avoid potential pollution, but also lead to a BA-laden BC (abbreviated as BA/BC) composite which may find applications in water treatment.

In this work, the BC pellicles were purified by a modified process without NaOH treatment, which yields the BA/BC composite. To achieve this, BC pellicles were repeatedly rinsed with deionized water such that the residual impurities can be removed while preserving the BA in the network of cellulose matrix. As a control, BC pellicles were purified via conventional procedures to remove both the residual impurities and BA, yielding the BC. The adsorption capacities of BC and BA/BC adsorbents with toxic heavy metal ions (including Pb(II), Cu(II), Ni(II), and Cr(VI)) in aqueous solutions were tested. In addition, the

* Corresponding author at: School of Materials Science and Engineering, Tianjin University, Tianjin 300072, China.
E-mail address: hlluotju@126.com (H. Luo).

https://doi.org/10.1016/j.compositesa.2019.105560
Received 30 April 2019; Received in revised form 11 July 2019; Accepted 29 July 2019
Available online 29 July 2019
1359-835X/

morphology and physicochemical properties of BA and BC were characterized.

2. Materials and methods

2.1. Materials

Yeast extract, tryptone, disodium phosphate (Na_2HPO_4), and acetic acid, provided by Beijing Innochem Science & Technology Co., Ltd., China, were used as received for BC production. The bacterial strain, *Komagataeibacter xylinus* X-2, was received from Tianjin University of Science and Technology, Tianjin, China. The heavy metal salts including $Pb(NO_3)_2$, $CuSO_4{\cdot}5H_2O$, $NiSO_4{\cdot}6H_2O$, and K_2CrO_4, and other chemicals were purchased from Tianjin Kemiou Chemical Reagent Co., Ltd., Tianjin, China.

2.2. Preparation of BA/BC and BC aerogels

The preparation process of BA/BC and BC pellicles was similar except that BA/BC did not experience hot NaOH treatment. The recipe of the medium culture was reported in our previous work [13,14], which consisted of 2.5% (w/v) glucose, 0.75% (w/v) yeast extract, 1% (w/v) tryptone, and 1% (w/v) Na_2HPO_4. The culture medium (pH = 4–5) was sterilized at 115 °C for 30 min followed by inoculation and incubation at 30 °C for 5 days.

To remove impurities such as residual nutrition components while preserving BA *in situ*, the harvested BC pellicles were soaked in deionized water which was renewed every 4 h until no color could be found in the water. Alternatively, other BC pellicles were treated with hot NaOH as described in our previous studies [13,15], leading to BC pellicles. Both BA/BC and BC pellicles were freeze dried using the procedures reported previously [16], yielding BA/BC and BC membranes, respectively.

2.3. Characterizations

The morphologies of BA/BC and BC were investigated by scanning electron microscopy (SEM, SU8010, Hitachi, Japan). The elemental analysis was carried out by energy dispersive X-ray spectroscopy (EDS) on a SEM-attached EDS instrument. X-ray diffraction (XRD) analysis was conducted to determine the crystalline structure of various scaffolds with a D8 Advance X-ray diffractometer using Cu-Kα radiation (λ = 0.154 nm). The crystallinity index (C_I) was calculated by Segal's method [17]. Fourier transform infrared spectroscopy (FTIR) in attenuated total reflectance (ATR) mode was performed using a Perkin-Elmer Spectrum One spectrometer. Adsorption of Pb(II) on BA/BC surface was confirmed by X-ray photoelectron spectroscopy (XPS) analysis.

Static mechanical tests including tensile and compressive were conducted using a micro-electromagnetic fatigue testing machine (MUF-1050, Tianjin Care Measure & Control Co., Ltd., Tianjin, China). The tensile measurement was conducted in accordance with ASTM Standard D638 and the compressive test was carried out according to the method reported by Chen et al. [18]. The dimensions of BC and BA/BC hydrogels were 25 mm × 10 mm × 1 mm and Ø20 mm × 7 mm, respectively, for tensile and compressive tests. The specimens for tensile test were cut with a blade from large hydrogels (50 mm × 40 mm × 1 mm) and the specimens for compressive tests were directly incubated in 12-well culture plates. The strain rate was 5 mm min^{-1} in both cases. At least five specimens were tested for each sample, and the averages and standard deviations were reported.

2.4. Adsorption experiments

Prior to adsorption experiments, stock solutions (1000 mg L^{-1}) of standardized Pb(II), Cu(II), Ni(II), and Cr(VI) were prepared by dissolving their salts in deionized water. The adsorption experiments were conducted by adding BC and BA/BC membranes (20 mg, 10 × 10 × 0.5 mm^3) in 50 mL solutions of metal ions at different concentrations (Cu(II): 100 mg L^{-1}, pH = 6; Ni(II): 50 mg L^{-1}, pH = 6; Cr (VI): 50 mg L^{-1}, pH = 2) and kept on a shaker for 60 min (T = 30 °C, R = 150 rpm). In the case of Pb(II), a given amount of BC and BA/BC membranes (ranging from 10 to 80 mg) was added into 50 mL of Pb(II) solutions at initial concentrations ranging from 50 to 1000 mg L^{-1} for up to 120 min. The pH of the final Pb(II) solution (pH = 1–6) was adjusted with diluted HNO_3 or NaOH. The BC membranes with adsorbed metal ions were removed and the decrease in ion concentration in the supernatant liquid was determined using an AA-6800 atomic absorption spectrophotometer (Shimadzu, Japan).

The adsorption capacity (q_e, mg g^{-1}, metal ion uptake at the equilibrium) of Pb(II), Cu(II), Ni(II), and Cr(VI) was calculated using the following equation:

$$q_e = \frac{(C_0 - C_e)V}{M} \quad (1)$$

where C_0 and C_e are the initial and residual concentration of adsorbate (mg L^{-1}), respectively. V (L) is the volume of the solution and M (g) is the dry mass of the adsorbent used in the experiments.

2.5. Desorption and regeneration experiments

For desorption of Pb(II), the BC and BA/BC adsorbents with Pb(II) were washed with deionized water and then stirred in 50 mL of 0.1 mol L^{-1} HCl at 30 °C for 4 h. After the desorption tests, the adsorbents were separated and washed with abundant deionized water, and re-used in the next cycle of adsorption experiments. The adsorption-desorption experiments were conducted for 5 cycles at pH 6 and an initial ion concentration of 200 mg L^{-1}.

All the adsorption experiments were conducted at least in triplicate under identical conditions.

After the 5th cycle of adsorption-desorption, the number of remained bacteria in the middle layer of BA/BC membrane was counted with the help of SEM (SU8010, Hitachi, Japan) by randomly selecting five regions under the SEM. The bacteria number of original BA/BC membrane was also measured using the same method.

3. Results and discussion

3.1. Morphology and structure

The photos of BA/BC and BC hydrogels and aerogels are shown in Fig. 1a. A minor difference in color between BC and BA/BC pellicles and aerogels is observed, the BA/BC pellicle being less transparent and the respective aerogel slightly darker due to the existence of BA. The morphology shown in Fig. 1b reveals a typical interconnected porous structure of BC, in line with our previous studies [10,11]. As shown in Fig. 1c, many bacterial cells are observed in the matrix of BC. A magnified image reveals the bundling of a bacterial cell by BC nanofibers (Fig. 1d). Such mechanical interaction is beneficial to the improvement of mechanical properties of BC.

The element mapping images (Fig. 2) show the shape of the BA, given the higher density of the C, O, and N elemental composition, as could be expected. The EDS results (Fig. S1, Supplementary Material) show an atomic nitrogen content of 14.3% in BA/BC while there is no detectable N in BC.

To determine the effect of purification on the crystalline structure, XRD measurement was conducted and the results are presented in Fig. 3a. Both materials show three diffraction peaks at 14.4°, 16.8°, and 22.7°, which corresponds to the crystalline planes of (1 $\bar{1}$ 0), (1 1 0), and (2 0 0), respectively [11,16,17]. Further analysis on the crystallinity index reveals obvious difference. The BC has a value of 91% while BA/BC has a lower value of 85%, assigned to the presence of BA.

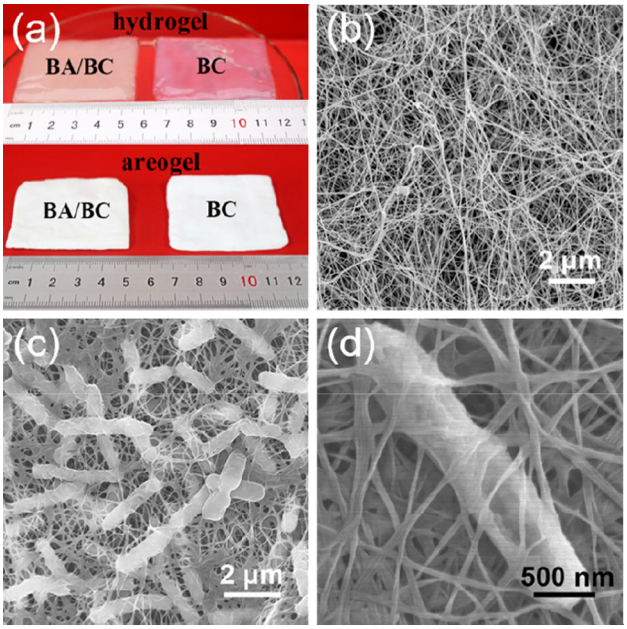

Fig. 1. Digital photos of (a) BA/BC and BC hydrogels and aerogels. SEM images of BC (b), BA/BC (c), and a bacterial cell in BC matrix (d). (For interpretation of the references to color in this figure legend, the reader is referred to the web version of this article)

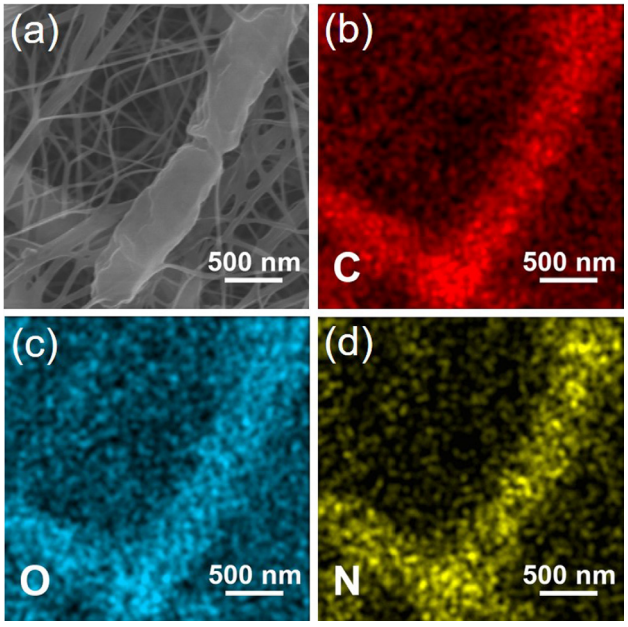

Fig. 2. Morphology (a) and elemental mapping images of C (b), O (c), and N (d) in BA/BC. (For interpretation of the references to color in this figure legend, the reader is referred to the web version of this article)

Then, the surface chemistry of BA/BC and BC materials was assessed. As shown in Fig. 3b, the peaks observed at 3620–3200 cm^{-1} and 1650 cm^{-1} in the FTIR spectra of BC and BA/BC can be attributed to hydroxyl groups and water present on the cellulosic fiber surface [19]. In addition, the band at 3022–2828 cm^{-1} is attributed to C—H stretching vibration. The bands at 1001–1271 cm^{-1} are assigned to the vibrations of C—O—C [20]. Compared with that of BC, a much stronger peak at 1650 cm^{-1} and a new peak at 1539 cm^{-1} in the spectrum of BA/BC can be observed, which can be ascribed to the vibration of amide I (C═O) and amide II (N—H) [21,22], respectively, resulting from the BA. The FTIR results confirm that BC contains large number of free hydroxyl groups on the surface while the presence of BA introduces extra amide groups to BA/BC, which are expected to be beneficial to the adsorption of metal ions.

3.2. Mechanical properties

Mechanical properties are important for fibrous aerogels in the removal of metal ions. Therefore, the mechanical properties of BA/BC and BC materials were tested under tensile and compressive loadings (Fig. 4 and Table S1, Supplementary Material). The tensile strain-stress curves of BC and BA/BC (Fig. 4a) indicate a higher maximum stress of BA/BC than BC while the strain at break reverses. The compressive strain-stress curves (Fig. 4b) reveal that BA/BC has a higher compressive strength than BC, consistent with the tensile properties. The obtained tensile and compressive properties are presented in Table S1. This finding suggests that the preservation of BA in cellulose matrix can lead to higher mechanical properties than bare BC.

George et al. reported that 0.1 M NaOH treatment reduced mechanical properties of BC [23]. This reduction was explained by the change of inter and intra molecular H-bonds between adjacent cellulose fibers, which caused fiber swelling. In contrast, Nishi et al. claimed that NaOH treatment improved mechanical properties [24]. Similarly, Gea et al. claimed that alkalization of BC using 2.5 wt% NaOH solution produced a twofold increase in Young's modulus, which was assigned to the removal of impurities, allowing better interactions among BC fibrils [7]. Although controversial claims were reported, overall, more studies seemed to support the improvements in mechanical properties of processed BC. In this study, BC was obtained after 30 min of 0.5 M NaOH treatment and all impurities and BA were removed. Therefore, BC is expected to show better mechanical properties than BA/BC. However, the opposite result is observed. The significantly improved mechanical properties of BA/BC and the SEM image shown in Fig. 1d suggest that another mechanism governs the improvements in mechanical properties of BA/BC, as schematically illustrated in Fig. 5: the presence of BA acts as reinforcing junctions which connect numerous cellulose nanofibers, resembling interlockers in a suspension bridge. These interlockers limit the deformation of the cellulose fibers, increase the rigidity of the structure, and thus improve mechanical properties of BA/BC over BC. This is a significant finding as it endows BC with high mechanical properties. Similar mechanisms have been reported by previous researchers. For instance, Yu et al. claimed that the abundant welded junctions (graphene) endowed the carbon aerogels with robust and stable mechanical performance [25] and Kim et al. believed that the crosslinking points or nodes in the carbon nanotube aerogel increased mechanical properties [26].

3.3. Adsorption capacities of BC and BA/BC

To preliminarily assess the effect of the presence of BA in BC on the adsorption of metal ions, adsorption assays of BA/BC and BC without surface functionalization were performed which may increase the adsorption capacity of cellulose [19,27]. Pb(II) was chosen as a model metal ion and the adsorption of BA/BC and BC under various conditions was assessed.

First, the adsorption capacities of BA/BC and BC were assessed as a function of cellulose dose (Fig. 6a). A continuous decrease in adsorption capacities is observed as the BC dose increases. This is simply due to the decreased number of free Pb(II) in the solution per adsorption site, as the adsorbent dose increases. BA/BC possesses significantly higher adsorption capacities. The maximum value of BA/BC (ca. 52 mg g^{-1}) is nearly 3.5 times that of BC (ca. 16 mg g^{-1}).

Then, the change in adsorption capacities with different initial metal ion concentrations was measured. As shown in Fig. 6b, initially, the increase in Pb(II) concentration leads to enhanced adsorption capacities. These improvements are attributed to the increased amount of Pb(II) which can be adsorbed by BC and BA/BC adsorbents. The

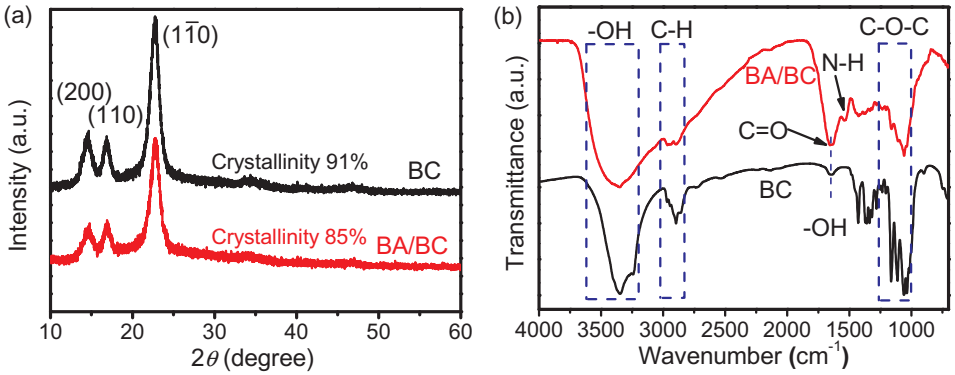

Fig. 3. XRD (a) and FTIR (b) spectra of BC and BA/BC. (For interpretation of the references to color in this figure legend, the reader is referred to the web version of this article)

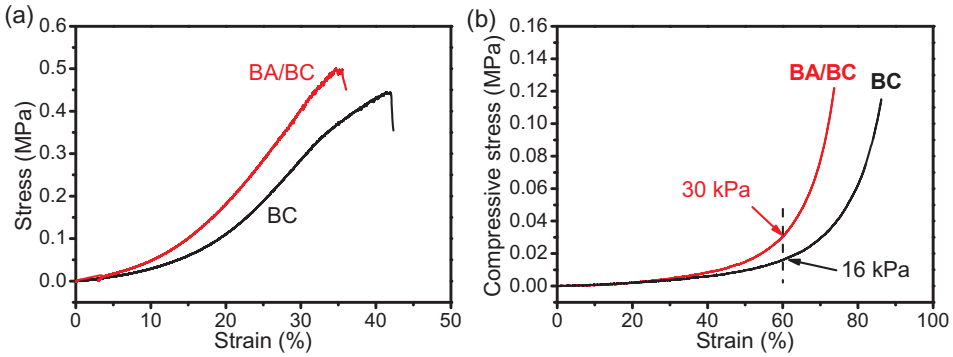

Fig. 4. Representative tensile (a) and compressive (b) stress-strain curves of BC and BA/BC. (For interpretation of the references to color in this figure legend, the reader is referred to the web version of this article)

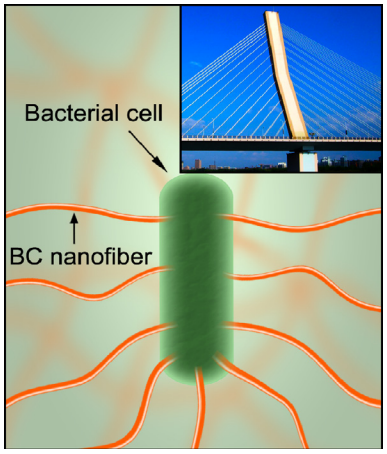

Fig. 5. A schematic illustration of the reinforcing effect of BA in BC matrix resembling interlockers in a suspension bridge. (For interpretation of the references to color in this figure legend, the reader is referred to the web version of this article)

adsorption capacities reach plateau values when initial ion concentration exceeds a threshold value (400 mg L^{-1} for BC and 200 mg L^{-1} for BA/BC).

Previous studies indicated that the adsorption of metal ions onto adsorbents is pH-dependent [28,29]. Therefore, the adsorption capacities of two BC materials were measured at varying pH values. Fig. 6c reveals that the adsorption of Pb(II) is less prominent at lower pH for both BC adsorbents. This trend can be explained as follows: The large amount of protons (H^+) in the strong acidity medium may compete with Pb(II) for hydroxyl groups, in both materials [30]; on the other hand, protonation of amide groups reduces the ability for coordination of Pb(II) in the BA/BC sample, resulting in a lower adsorption at a lower pH [31].

Finally, the adsorption of Pb(II) by BC and BA/BC was measured as a function of time (Fig. 6d). As expected, the adsorption capacities show a rapid initial increase in the first 60 min and then reach equilibrium. This is a common pattern for many adsorbents towards various metal ions [32], which is explained by the limitation of available active sites on the surface of adsorbents.

It is clearly noted that BA/BC has significantly higher adsorption capacities to Pb(II) as compared to BC regardless of the adsorption conditions. It is noticed that although the maximum adsorption capacity of BA/BC (*ca.* 52 mg g^{-1}) is comparable to the carboxymethylated BC [28], it is lower than some adsorbents using BA and other BC-based materials, as presented in Table S2 [28,31–35], which is simply due to the lack of surface functionalization as mentioned above.

To determine the recyclability of BC and BA/BC adsorbents, adsorption and desorption experiments were conducted for 5 cycles. The results in Fig. S2 (Supplementary Material) demonstrate that more than 85% of their initial adsorption capacities is maintained after the 5th adsorption cycle, suggesting both BC and BA/BC are recyclable. In addition, the bacterial number in the middle layer of BA/BC membrane was determined before and after adsorption-desorption cycles. The bacterial number decreases from 39583 mm^{-2} to 30417 mm^{-2} after 5 adsorption-desorption cycles, showing a retention of around 77%. However, the tensile strength of BA/BC does not significantly change after 5 cycles.

Besides Pb(II), the adsorption of both BC adsorbents to Cu(II), Ni(II), and Cr(VI) was also assessed and it is found that in all cases (Fig. S3, Supplementary Material), BA/BC shows significantly higher adsorption capacities than BC.

The significant improvements in BA/BC performance as an

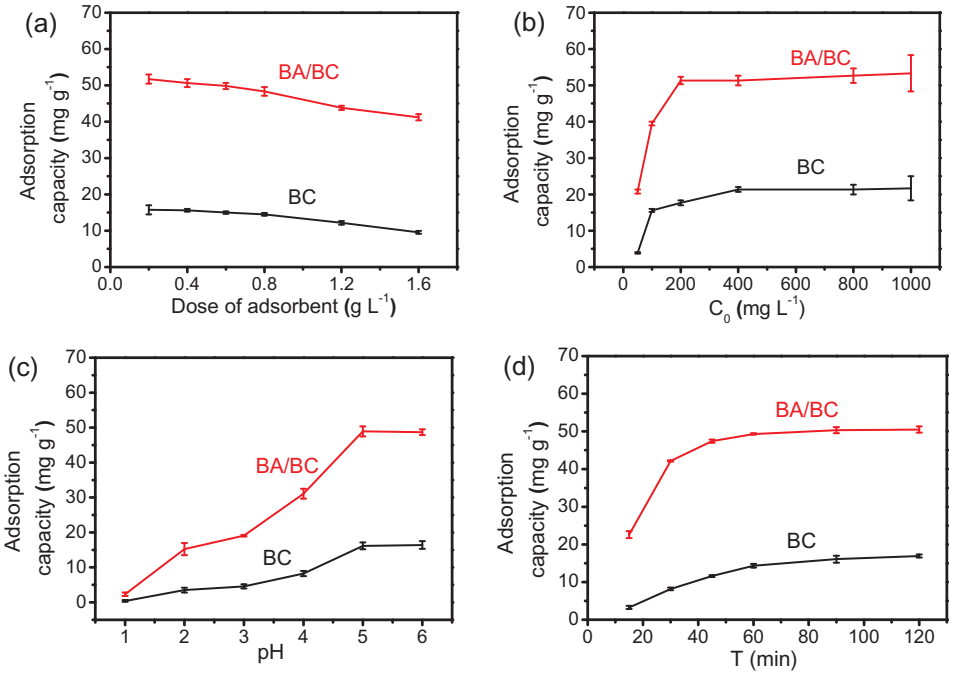

Fig. 6. Dependence of adsorption capacities of BA/BC and BC to Pb(II) on adsorbent dose (a), initial Pb(II) concentration (b), pH (c), and adsorption time (d). (For interpretation of the references to color in this figure legend, the reader is referred to the web version of this article)

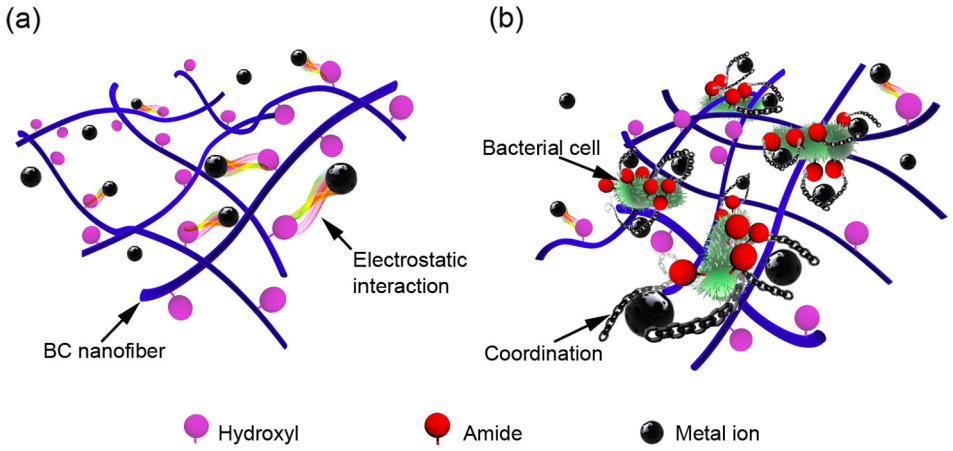

Fig. 7. The proposed adsorption mechanisms for the adsorption of BA/BC and BC to metal ions. (For interpretation of the references to color in this figure legend, the reader is referred to the web version of this article)

adsorbent can be explained as follows: It has been accepted that mechanisms involved in the sorption process of cellulose materials generally include ion exchange, coordination, microprecipitation, and surface adsorption [36]. FTIR results and adsorption performances of BC may indicate that the dominant mechanism involved in BC is the electrostatic interaction mechanism between metal ions and functional groups of BC adsorbents. This mechanism can be proved by the reduced adsorption of metal ions with increasing acid concentration due to the increase in concentration of competitive proton [36]. In this case, the adsorption capacity depends on the number and activity of the surface groups. There are a large number of hydroxyl groups on BC, which dominate the electrostatic interaction with metal ions. However, its weak activity results in low adsorption capacities to various metal ions [32,36]. This can elucidate the low adsorption capacities of BC. In the case of BA/BC, there is another mechanism, the coordination mechanism [19]. It has been reported that soft ions such as Cd(II), Cu(II), and Pb(II) can be bound to amide available on the BA, by coordination [31,37,38]. Obviously, there are no amide groups on BC while they are present on BA/BC, which is in agreement with the report that there are several chemical groups that would attract the metal ions in biomass such as amino, phosphate, and amide groups [39]. Accordingly, the presence of amide groups on BA/BC contributes to the improved adsorption capacities to Pb(II), Cu(II), Ni(II), and Cr(VI). In conclusion, the presence of amide groups on BA/BC enhances its adsorption ability towards heavy metal ions. The proposed mechanisms are schematically illustrated in Fig. 7.

To confirm the adsorption of metal ions on BC and BA/BC materials and understand the mechanism of Pb(II) adsorption, XPS analysis was conducted using Pb(II)-adsorbed adsorbent materials as models since XPS can identify the interaction of a metal ion with the surface chemical groups on an adsorbent [40]. The survey spectra (Fig. 8a and b and Fig. S4, Supplementary Material) reveal the presence of Pb on the surface of the BC and BA/BC adsorbents. A comparison between Fig. 8a and b evidences the larger amount of adsorbed Pb(II) in the BA/BC than the BC. High-resolution XPS spectrum of N 1s (Fig. 8c) demonstrates a peak at 398.3 eV, which is attributed to N—H bond. This N—H peak

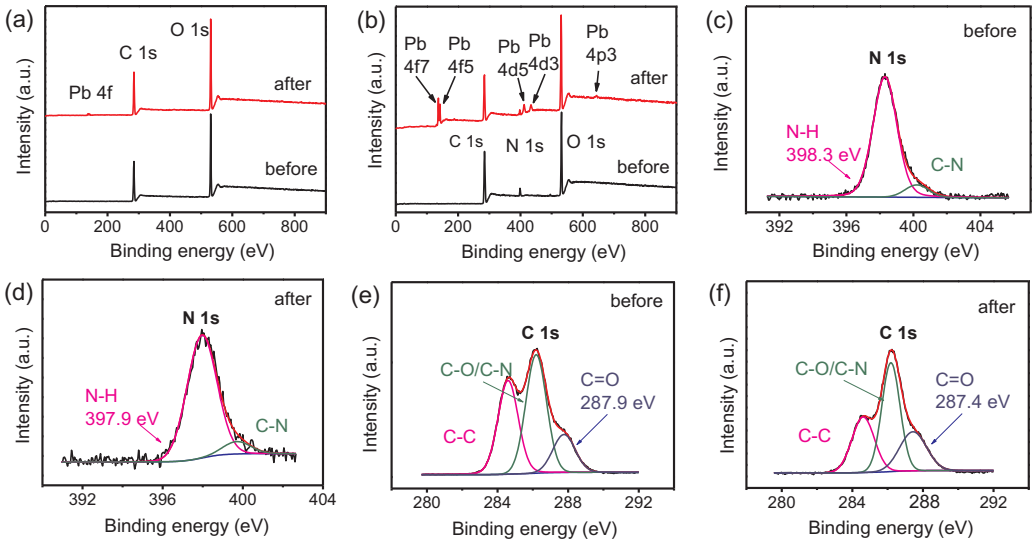

Fig. 8. XPS analysis results: (a and b) XPS wide-scan spectra of BC (a) and BA/BC (b) before and after adsorption of Pb(II); (c and d) High-resolution scan of N 1s in BA/BC before (c) and after (d) Pb(II) adsorption; (e and f) High-resolution scan of C 1s in BA/BC before (e) and after (f) Pb(II) adsorption. (For interpretation of the references to color in this figure legend, the reader is referred to the web version of this article)

shows a right shift to lower binding energy of 397.9 eV (Fig. 8d). The decreased binding energy upon Pb(II) adsorption is attributed to the formation of coordination bond of N-Pb(II) such that the N atoms share electrons with Pb(II), leading to reduced electron densities of N atoms [31,41,42]. Similarly, a decreased binding energy (from 287.9 to 287.4 eV) for C═O is observed in the high-resolution XPS spectrum of C 1s for BA/BC after adsorption (Fig. 8e and f). Therefore, the XPS results further confirm the coordination interaction between amide bond and metal ions on BA/BC, which greatly increases the adsorption capacities of BA/BC to heavy metal ions.

Although the adsorption kinetics and isotherms were not studied in this work, which will be the focus of our future investigation, the results presented in this paper are sufficient to confirm the significant role of BA reserved in BC in improving the adsorption capacities and mechanical properties of BA/BC.

4. Conclusions

In summary, a new BA/BC composite has been fabricated by the modified biosynthesis process without NaOH treatment. SEM images demonstrated the presence of many BA embedded in BA/BC. Mechanical tests confirmed that BA/BC showed improved mechanical properties over BC which experienced hot NaOH treatment. These improvements were ascribed to the presence of BA embedded in the BC matrix which acted as junctions to unite BC nanofibers together. When used as an adsorbent, the BA/BC showed significantly higher adsorption capacities than the BC due to the presence of amide groups in BA. These amide groups served as reactive sites to react with metal ions via coordination interaction. These results demonstrated that the preservation of BA in BC matrix made the fabrication process simpler, faster, and green, and the resultant BA/BC adsorbent was stronger and more efficient. This strategy will pave a new way for the development of a new BC composite with better properties than the BC prepared by traditional method.

Acknowledgements

Y Wan and J Wang contributed equally to this work. This work was supported by the National Natural Science Foundation of China (Grant nos. 31870963, 51572187, and 51563008), and the Key Project of Natural Science Foundation of Jiangxi Province (Grant no. 20161ACB20018).

Appendix A. Supplementary material

Supplementary data to this article can be found online at https://doi.org/10.1016/j.compositesa.2019.105560.

References

[1] Irvin CW, Satam CC, Meredith JC, Shofner ML. Mechanical reinforcement and thermal properties of PVA tricomponent nanocomposites with chitin nanofibers and cellulose nanocrystals. Composites Part A 2019;116:147–57.
[2] Kroeling H, Duchemin B, Dormanns J, Schabel S, Staiger MP. Mechanical anisotropy of paper-based all-cellulose composites. Composites Part A 2018;113:150–7.
[3] Zhan Y, Xiong C, Yang J, Shi Z, Yang Q. Flexible cellulose nanofibril/pristine graphene nanocomposite films with high electrical conductivity. Composites Part A 2019;119:119–26.
[4] Stumpf TR, Yang X, Zhang J, Cao X. In situ and ex situ modifications of bacterial cellulose for applications in tissue engineering. Mater Sci Eng C 2016;82:372–83.
[5] Jozala AF, de Lencastre-Novaes LC, Lopes AM, De CS-EV, Mazzola PG, Pessoa-Jr A, et al. Bacterial nanocellulose production and application: a 10-year overview. Appl Microbiol Biotechnol 2016;100(5):2063–72.
[6] Klemm D, Schumann D, Udhardt U, Marsch S. Bacterial synthesized cellulose–artificial blood vessels for microsurgery. Prog Polym Sci 2001;26(9):1561–603.
[7] Gea S, Reynolds CT, Roohpour N, Wirjosentono B, Soykeabkaew N, Bilotti E, et al. Investigation into the structural, morphological, mechanical and thermal behaviour of bacterial cellulose after a two-step purification process. Bioresour Technol 2011;102(19):9105–10.
[8] McKenna BA, Mikkelsen D, Wehr JB, Gidley MJ, Menzies NW. Mechanical and structural properties of native and alkali-treated bacterial cellulose produced by Gluconacetobacter xylinus strain ATCC 53524. Cellulose 2009;16(6):1047–55.
[9] Luo H, Dong J, Zhang Y, Li G, Guo R, Zuo G, et al. Constructing 3D bacterial cellulose/graphene/polyaniline nanocomposites by novel layer-by-layer in situ culture toward mechanically robust and highly flexible freestanding electrodes for supercapacitors. Chem Eng J 2018;334:1148–58.
[10] Luo H, Dong J, Yao F, Yang Z, Li W, Xu X, et al. Layer-by-layer assembled bacterial cellulose/graphene oxide hydrogels with extremely enhanced mechanical properties. Nano Micro Lett 2018;10(3):42.
[11] Luo H, Dong J, Xu X, Wang J, Yang Z, Wan Y. Exploring excellent dispersion of graphene nanosheets in three-dimensional bacterial cellulose for ultra-strong nanocomposite hydrogels. Composites Part A 2018;109:290–7.
[12] Benitez AJ, Walther A. Cellulose nanofibril nanopapers and bioinspired nanocomposites: a review to understand the mechanical property space. J Mater Chem A 2017;5(31):16003–24.
[13] Wan YZ, Huang Y, Yuan CD, Raman S, Zhu Y, Jiang HJ, et al. Biomimetic synthesis of hydroxyapatite/bacterial cellulose nanocomposites for biomedical applications. Mater Sci Eng C 2007;27(4):855–64.
[14] Luo H, Ao H, Li G, Li W, Xiong G, Zhu Y, et al. Bacterial cellulose/graphene oxide nanocomposite as a novel drug delivery system. Curr Appl Phys 2017;17(2):249–54.
[15] Wan Y, Hu D, Xiong G, Li D, Guo R, Luo H. Directional fluid induced self-assembly of oriented bacterial cellulose nanofibers for potential biomimetic tissue engineering scaffolds. Mater Chem Phys 2015;149(7):1–5.
[16] Si H, Luo H, Xiong G, Yang Z, Raman SR, Guo R, et al. One-step in situ biosynthesis of graphene oxide-bacterial cellulose nanocomposite hydrogels. Macromol Rapid Commun 2014;35(9):1706–11.
[17] Segal L, Creely JJ, Martin AE, Conrad CM. An empirical method for estimating the degree of crystallinity of native cellulose using the X-ray diffractometer. J Text Res 1959;29(10):786–94.

[18] Chen W, Ma J, Zhu L, Morsi Y, Hany E-H, Al-Deyab SS, et al. Superelastic, superabsorbent and 3D nanofiber-assembled scaffold for tissue engineering. Colloid Surf B Biointerf 2016;142:165–72.
[19] Setyono D, Valiyaveettil S. Functionalized paper-a readily accessible adsorbent for removal of dissolved heavy metal salts and nanoparticles from water. J Hazard Mater 2016;302:120–8.
[20] Feng Y, Zhang X, Shen Y, Yoshino K, Feng W. A mechanically strong, flexible and conductive film based on bacterial cellulose/graphene nanocomposite. Carbohyd Polym 2012;87(1):644–9.
[21] Deng S, Ting YP. Characterization of PEI-modified biomass and biosorption of Cu (II), Pb(II) and Ni(II). Water Res 2005;39(10):2167–77.
[22] Deng S, Ting YP. Polyethylenimine-modified fungal biomass as a high-capacity biosorbent for Cr(VI) anions: sorption capacity and uptake mechanisms. Environ Sci Technol 2005;39(21):8490–6.
[23] George J, Ramana KV, Sabapathy SN, Bawa AS. Physico-mechanical properties of chemically treated bacterial (Acetobacter xylinum) cellulose membrane. World J Microb Biot 2005;21(8–9):1323–7.
[24] Nishi Y, Uryu M, Yamanaka S, Watanabe K, Kitamura N, Iguchi M, et al. The structure and mechanical properties of sheets prepared from bacterial cellulose. J Mater Sci 1990;25(6):2997–3001.
[25] Yu Z-L, Qin B, Ma Z-Y, Huang J, Li S-C, Zhao H-Y, et al. Superelastic hard carbon nanofiber aerogels. Adv Mater 2019;31(23):1900651.
[26] Kim KH, Oh Y, Islam M. Graphene coating makes carbon nanotube aerogels superelastic and resistant to fatigue. Nat Nanotech 2012;7(9):562.
[27] Bethke K, Palantöken S, Andrei V, Roß M, Raghuwanshi VS, Kettemann F, et al. Functionalized cellulose for water purification, antimicrobial applications, and sensors. Adv Funct Mater 2018;28(23):1–14.
[28] Chen S, Zou Y, Yan Z, Shen W, Shi S, Zhang X, et al. Carboxymethylated-bacterial cellulose for copper and lead ion removal. J Hazard Mater 2009;161(2):1355–9.
[29] Khan MN, Wahab MF. Characterization of chemically modified corncobs and its application in the removal of metal ions from aqueous solution. J Hazard Mater 2007;141(1):237–44.
[30] Yan L, Zhao Q, Jiang T, Liu X, Li Y, Fang W, et al. Adsorption characteristics and behavior of a graphene oxide-Al 13 composite for cadmium ion removal from aqueous solutions. RSC Adv 2015;5(83):67372–9.
[31] Luo S, Li X, Chen L, Chen J, Wan Y, Liu C. Layer-by-layer strategy for adsorption capacity fattening of endophytic bacterial biomass for highly effective removal of heavy metals. Chem Eng J 2014;239(1):312–21.
[32] Jin X, Xiang Z, Liu Q, Chen Y, Lu F. Polyethyleneimine-bacterial cellulose bioadsorbent for effective removal of copper and lead ions from aqueous solution. Bioresour Technol 2017;244:844–9.
[33] Huang X, Zhan X, Wen C, Xu F, Luo L. Amino-functionalized magnetic bacterial cellulose/activated carbon composite for Pb^{2+} and methyl orange sorption from aqueous solution. J Mater Sci Technol 2018;34(5):855–63.
[34] Shen W, Chen S, Shi S, Li X, Zhang X, Hu W, et al. Adsorption of Cu(II) and Pb(II) onto diethylenetriamine-bacterial cellulose. Carbohyd Polym 2009;75(1):110–4.
[35] Zhu H, Jia S, Wan T, Jia Y, Yang H, Li J, et al. Biosynthesis of spherical Fe_3O_4/bacterial cellulose nanocomposites as adsorbents for heavy metal ions. Carbohyd Polym 2011;86(4):1558–64.
[36] Hokkanen S, Bhatnagar A, Sillanpää M. A review on modification methods to cellulose-based adsorbents to improve adsorption capacity. Water Res 2016;91:156–73.
[37] Heidari A, Younesi H, Mehraban Z. Removal of Ni(II), Cd(II), and Pb(II) from a ternary aqueous solution by amino functionalized mesoporous and nano mesoporous silica. Chem Eng J 2009;153(1–3):70–9.
[38] Vukovic GD, Marinkovic AD, Skapin SD, Ristic MD, Aleksic R, Peric-Grujic AA, et al. Removal of lead from water by amino modified multi-walled carbon nanotubes. Chem Eng J 2011;173(3):855–65.
[39] Ahluwalia SS, Goyal D. Microbial and plant derived biomass for removal of heavy metals from wastewater. Bioresour Technol 2007;98(12):2243–57.
[40] Deng SB, Bai RB, Chen JP. Aminated polyacrylonitrile fibers for lead and copper removal. Langmuir 2003;19(12):5058–64.
[41] Huang J, Ye M, Qu Y, Chu L, Chen R, He Q, et al. Pb (II) removal from aqueous media by EDTA-modified mesoporous silica SBA-15. J Colloid Interf Sci 2012;385(1):137–46.
[42] Zhu Y, Hu J, Wang J. Competitive adsorption of Pb(II), Cu(II) and Zn(II) onto xanthate-modified magnetic chitosan. J Hazard Mater 2012;221:155–61.